The significance of the number of periods and period size in 2D photonic crystal waveguides

Mirsaeid Sarollahi[a], Jonathan Mishler[b], Stephen J. Bauman[a,c], Salvador Barraza-Lopez[a,b] , Paul Millett[a,d] , Joseph B. Herzog[*,a,b,c]

[a]Microelectronics-Photonics Program, University of Arkansas, Fayetteville, AR, 72701, USA;
[b]Department of Physics, University of Arkansas, Fayetteville, AR, 72701, USA;
[c]Institute for Nanoscience and Engineering, University of Arkansas, Fayetteville, AR 72701, USA
[d] Mechanical Engineering Department, University of Arkansas, Fayetteville, AR 72701, USA

ABSTRACT

This work investigates the significance of the number of periods in two-dimensional photonic crystals. Models have been developed to study various photonic crystal properties (Reflection, Photonic crystal band gap). The numbers of photonic crystal periods, length of periods, and material properties have been investigated to determine their effect on the losses in the waveguide. The model focuses on a square period and has been designed to study transmission properties and the effects of period length. A finite difference frequency domain (FDFD) model has also been created to calculate the photonic band structure. Additionally, a simplified study focuses on the transmission of light through photonic crystal layers.

Keywords: Photonic crystal, Nano optics, 2D, periods, finite difference frequency domain, FDFD, Photonic Band Gap

1. INTRODUCTION

Photonic crystals (PCs) are periodic structures of dielectric material that can reflect, bend, and control light efficiently due to optical interference effects. PCs have forbidden optical energy bands that are known as photonic band gaps (PBGs) [1]. Applications of PCs are low-threshold lasers[2] , single-mode LEDs[3], [4], Bragg mirrors[5]–[7], optical filters[8]–[10], and efficient planar antennas[11], [12] . The fabrication of low loss photonic crystals[13], [14] has recently been evaluated for silicon based materials[15]–[20]. Also, biological photonic crystals have been characterized[21]–[25]. Photonic crystals that are periodic in two dimensions (2D) can guide light in two directions. The propagated light inside the photonic crystal structure is affected mainly by material properties (refractive index) and the periodicity of the crystal structure. In addition, the direction of light polarization and wavelength have a significant effect on reflectivity of the photonic crystal waveguide[26]–[28] .

This work is motivated by the possibility of inexpensively fabricating 2D photonic crystals with block copolymers [29]. Block copolymers can exhibit limitations on the number of perfect periods in a 2D structure and the size of these periods; therefore, this work will investigate these parameters. This work has two models. First, a finite element method (FEM) model was used to create reflection spectra in 2D PC layers. Next a finite difference frequency domain (FDFD) model was created to confirm the FEM results as well as to determine the entire photonic band structure for the device.

2. FEM MODEL

Reflection spectra from various PC configurations were calculated with a finite element model (COMSOL). The model, shown in Figure 1(a), is a periodic structure model has been created with variable parameters. This model has been developed to study the effect of these parameters, especially the number of periods and the period size. Polarization studies have also been investigated as well as inverting the material structure of the device so that the crystal is either a GaAs slab with air holes, or an array of GaAs posts in air. The reflection spectrum has been determined for both transverse electric (TE) and transverse magnetic (TM) polarization directions.

* Email: jbherzog@uark.edu

Nanoengineering: Fabrication, Properties, Optics, and Devices XII, edited by Eva M. Campo, Elizabeth A. Dobisz, Louay A. Eldada, Proc. of SPIE Vol. 9556, 95561B · © 2015 SPIE · CCC code: 0277-786X/15/$18 · doi: 10.1117/12.2188321

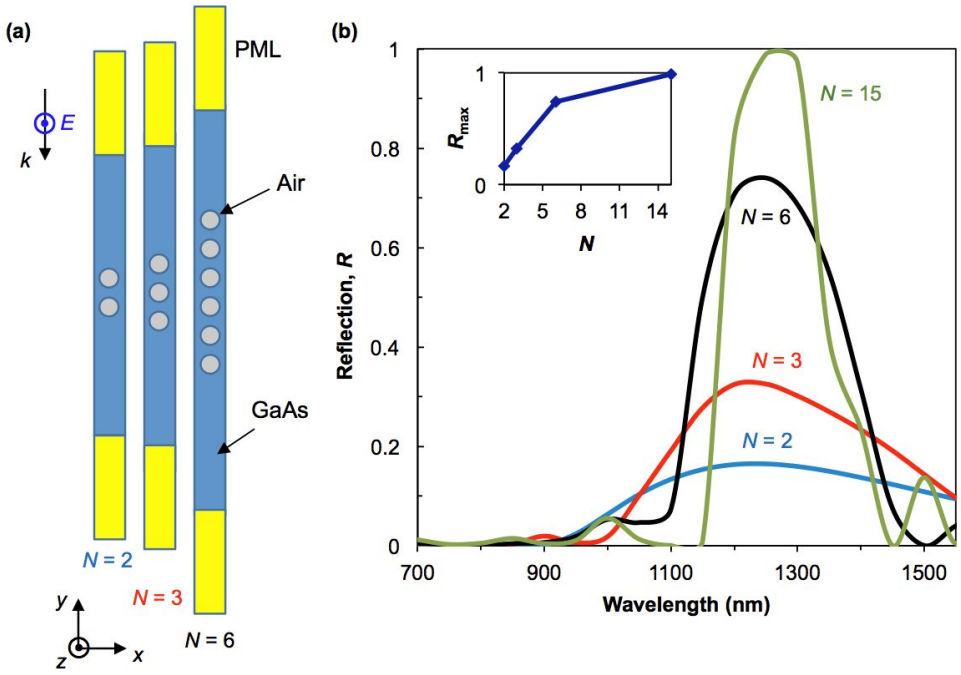

Figure 1. (a) Geometry of model. Perfectly matched layers (PMLs) are at the top and bottom of the geometry. The PC was modeled as a GaAs slab with air holes. The region shown was modeled to have left and right edges that are infinitely periodic. The number of vertical periods (N) can be changed as shown. The incident light direction (k) and polarization direction (E) are labeled relative to the model. (b) Reflection spectra for different values of N. The photonic band gap is seen with a central peak around 1250 nm. The inset plots the intensity of the reflection as the number of periods increases. The period of the model in this figure is $P = 200$ nm.

The model consists of a vertical unit cell that is periodic in one dimension, both the –x and +x directions, as labeled in Figure 1(a). In the y-direction, the number of periods, N, was varied. Light is incident in the $-y$ direction. The 2D photonic crystal had a square lattice. The materials studied in this work were either a GaAs substrate with air holes of GaAs posts in air. The length of the rectangle was function of the number of spots layers inside the rectangle so that the distance between the incident light port and the photonic crystal was always four times the period, $4P$. Incident light could be polarized in both the TE and TM mode directions.

3. RESULTS

Figure 1(b) shows how the reflection spectrum changes as a function the number of vertical periods, N. This model was for air holes in GaAs and has a constant period (hole center-to-center distance) of $P = 200$ nm. Incident light was polarized in the z-direction, which is also known as the transverse magnetic (TM) mode for photonic crystals[30]. As the number of periods (N) was increased, the reflection increased for the PBG wavelengths. The inset plots the maximum reflection at the PBG as a function of N. The reflection magnitude for $N = 2$ was less than 20% and for $N = 15$ was close to 100%.

Next, Figure 2 shows the polarization dependence of the PC. The constant parameters for this test were $N = 15$ and $P = 200$ nm with air holes in GaAs. Only the polarization was changed for this figure with the incident light being polarized in x (a), which is the transverse electric (TE) mode, and polarized in z (b), the TM mode. The wavelength range of the PBG was found to increase for the TE mode in comparison with the TM mode. The PBG wavelength range for the TE mode was approximately 500 nm while for the TM mode this range was approximately 300 nm.

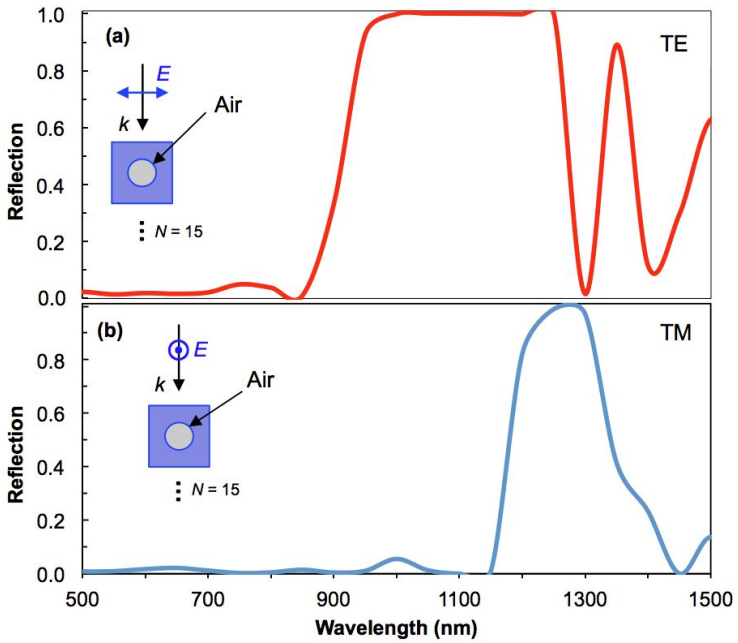

Figure 2. Effects of polarization on the PBG. Reflection spectrum for (a) TE mode and (b) TM mode with N = 15 and P = 200 nm.

The effects of material properties on the PBG were also investigated, as seen in Figure 3. GaAs posts in air showed a wider PBG wavelength range than air holes in GaAs. The PBG wavelength range for GaAs posts was 500 nm, while for air holes it was 300 nm. The reflection magnitude for GaAs posts was greater than for air holes. Another result was that the reflection magnitude at short wavelengths is greater for GaAs posts than air holes.

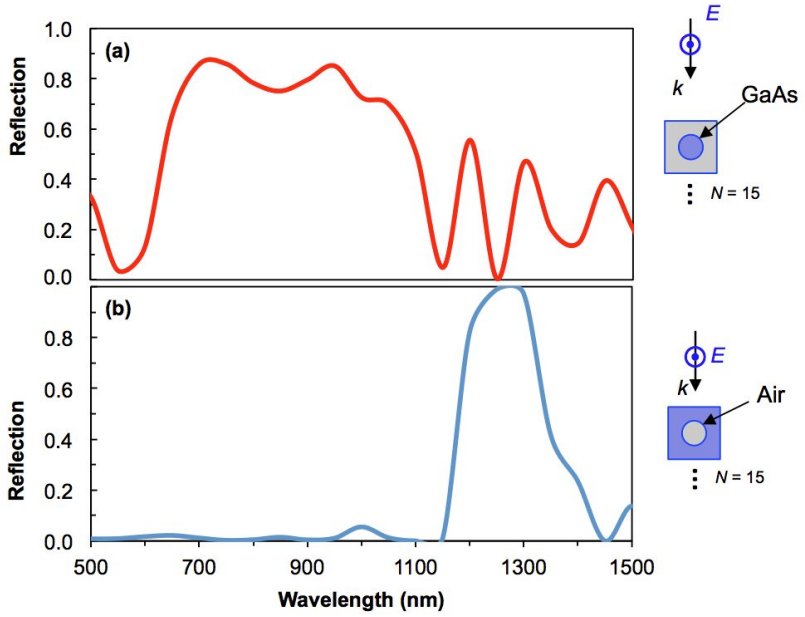

Figure 3. Effects of material properties on PBG. Reflection spectrum for a PC with (a) GaAs posts in air and (b) Air holes in GaAs. Constant parameters are incident light direction, polarization, and N = 15 and P = 200 nm.

The FEM was lastly used to plot the PBG peak shift as a function of the PC period. The period was changed from 200 to 300 nm and the results are shown in Figure 4. As P increases, so does the PBG central wavelength. This trend is plotted in the inset of Figure 4; it shows that peak increases linearly with *P*.

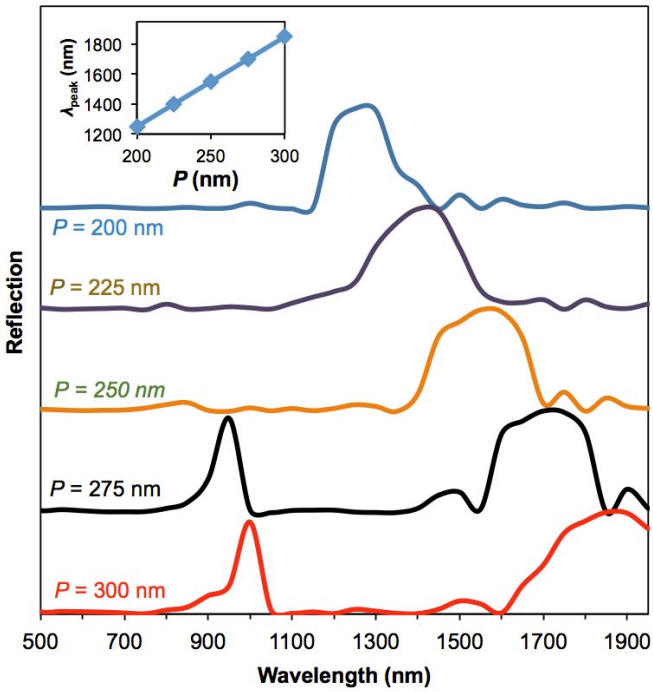

Figure. 4. Reflection spectrum for various PCs with different periods (*P*). Constant variable for this figure are *N* = 15 TM polarization with a PC with air holes surrounded by GaAs.

4. FINITE DIFFERENCE FREQUENCEY DOMAIN

Next, to get a complete picture of the photonic band structure, a FDFD method was used. In the following section, outlined is a FDFD method to calculate the photonic band which is similar to previous work [30], [31]. It begins with the commonly known set of Maxwell's equations:

$$\nabla \cdot \mathbf{B}(\mathbf{r},t) = 0 \tag{1}$$

$$\nabla \cdot \mathbf{D}(\mathbf{r},t) = \rho \tag{2}$$

$$\nabla \times \mathbf{E}(\mathbf{r},t) + \frac{\partial \mathbf{B}(\mathbf{r},t)}{\partial t} = 0 \tag{3}$$

$$\nabla \times \mathbf{H}(\mathbf{r},t) - \frac{\partial \mathbf{D}(\mathbf{r},t)}{\partial t} = \mathbf{J}. \tag{4}$$

Next, it is assumed that there are no free charges or currents, which require that both $\rho = 0$ and $\mathbf{J} = 0$. It is further assumed that the materials in the model are linear, isotropic, non-magnetic ($\mu_r = 1$), and frequency independent, and that the permittivity $\varepsilon = \varepsilon_0\varepsilon_r$ is real and positive.[†] Therefore, the constitutive relationships show that

$$\mathbf{B}(\mathbf{r},t) = \mu_0\mu_r\mathbf{H}(\mathbf{r},t) \tag{5}$$

$$\mathbf{D}(\mathbf{r},t) = \varepsilon_0\varepsilon_r(\mathbf{r})\mathbf{E}(\mathbf{r},t). \tag{6}$$

[†] ε_0 is the permittivity of free space and ε_r is the relative permittivity (or dielectric constant)

Factoring out the unnecessary constants and noting that $\mu_r = 1$, Maxwell's equations reduce to

$$\nabla \cdot \mathbf{H}(\mathbf{r},t) = 0 \tag{7}$$

$$\nabla \cdot \varepsilon_r(\mathbf{r})\mathbf{E}(\mathbf{r},t) = 0 \tag{8}$$

$$\nabla \times \mathbf{E}(\mathbf{r},t) + \mu_0 \frac{\partial \mathbf{H}(\mathbf{r},t)}{\partial t} = 0 \tag{9}$$

$$\nabla \times \mathbf{H}(\mathbf{r},t) - \varepsilon_0 \varepsilon_r(\mathbf{r}) \frac{\partial \mathbf{E}(\mathbf{r},t)}{\partial t} = 0. \tag{10}$$

The magnetic and electric fields are rewritten, to enforce the Bloch wave requirement, as

$$\mathbf{H}(\mathbf{r},t) = \mathbf{H}(\mathbf{r})e^{-i\omega t} \tag{11}$$

$$\mathbf{E}(\mathbf{r},t) = \mathbf{E}(\mathbf{r})e^{-i\omega t} \tag{12}$$

and derivatives computed, simplifying Maxell's equations even further:

$$\nabla \cdot \mathbf{H}(\mathbf{r}) = 0 \tag{13}$$

$$\nabla \cdot \varepsilon_r(\mathbf{r})\mathbf{E}(\mathbf{r}) = 0 \tag{14}$$

$$\nabla \times \mathbf{E}(\mathbf{r}) - i\omega\mu_0 \mathbf{H}(\mathbf{r}) = 0 \tag{15}$$

$$\nabla \times \mathbf{H}(\mathbf{r}) + i\omega\varepsilon_0\varepsilon_r(\mathbf{r})\mathbf{E}(\mathbf{r}) = 0. \tag{16}$$

Equations (13) and (14) require that the electromagnetic fields are transverse since there are no point sources or sinks. Equations (15) and (16) are then manipulated to give a single equation. By first solving for $\mathbf{H}(\mathbf{r})$ in Equation (15):

$$\mathbf{H}(\mathbf{r}) = \frac{\nabla \times \mathbf{E}(\mathbf{r})}{i\omega\mu_0} \tag{17}$$

and then substituting it into Equation (16):

$$\nabla \times \frac{\nabla \times \mathbf{E}(\mathbf{r})}{i\omega\mu_0} + i\omega\varepsilon_0\varepsilon_r(\mathbf{r})\mathbf{E}(\mathbf{r}) = 0 \tag{18}$$

$$\nabla \times \nabla \times \mathbf{E}(\mathbf{r}) = \omega^2\mu_0\varepsilon_0\varepsilon_r(\mathbf{r})\mathbf{E}(\mathbf{r}) \tag{19}$$

$$\nabla \times \nabla \times \mathbf{E}(\mathbf{r}) = \left(\frac{\omega}{c}\right)^2 \varepsilon_r(\mathbf{r})\mathbf{E}(\mathbf{r}) \tag{20}$$

the final desired result is obtained, since $c^2 = 1/(\varepsilon_0\mu_0)$. Equation (20) is an eigenvalue problem that can be solved using an FDFD scheme by first setting up a mesh along the desired geometry and calculating the relevant k-vectors along the geometry's irreducible Brillouin zone.

Next, Equation (20) is simplified using the curl of curl identity:

$$\nabla\big(\nabla \cdot \mathbf{E}(\mathbf{r})\big) - \nabla^2\mathbf{E}(\mathbf{r}) = \left(\frac{\omega}{c}\right)^2 \varepsilon_r(\mathbf{r})\mathbf{E}(\mathbf{r}). \tag{21}$$

Now recall that from the transverse requirement (Equation (14)),

$$\nabla \cdot \mathbf{E}(\mathbf{r}) = 0 \tag{22}$$

which simplifies Equation (21) to:

$$-\nabla^2\mathbf{E}(\mathbf{r}) = \left(\frac{\omega}{c}\right)^2 \varepsilon_r(\mathbf{r})\mathbf{E}(\mathbf{r}). \tag{23}$$

Expressing Equation (23) in terms of second order central finite differences gives the following:

$$-\left(\frac{E^x_{i+1,j}-2E^x_{i,j}+E^x_{i-1,j}}{h_x^2},\frac{E^y_{i,j+1}-2E^y_{i,j}+E^y_{i,j-1}}{h_y^2},0\right)=\left(\frac{\omega}{c}\right)^2\varepsilon_{r\,i,j}\left(E^x_{i,j},E^y_{i,j},0\right) \quad (24)$$

where h_x and h_x are the physical distances between the mesh elements along the x and y axis, respectively. Equation (24) is fully decoupled, that is changes in E_x only happen along i (x-axis), and changes in E_y only happen along j (y-axis), which therefore permits it to be rewritten as:

$$-\left(\frac{E_{i+1,j}-2E_{i,j}+E_{i-1,j}}{h_x^2}+\frac{E_{i,j+1}-2E_{i,j}+E_{i,j-1}}{h_y^2}\right)=\left(\frac{\omega}{c}\right)^2\varepsilon_{r\,i,j}E_{i,j}. \quad (25)$$

Finally, periodic boundary conditions are applied to the resulting FDFD matrix, which allow the desired eigenvalue problem to be solved computationally. Once the eigenvalues are calculated, they are multiplied by c^2 and rooted to isolate the eigenmodes, ω, which are then normalized.

Figure 5 shows an example of the $n\times n$ mesh in which the electric field at each position is labeled E_n. In the finite differences equation, the field at a given position, $E_{i,j}$, corresponds to one position, E_n. The $E_{i\pm1}$ and $E_{j\pm1}$ terms correspond to adjacent mesh cells in the lattice.

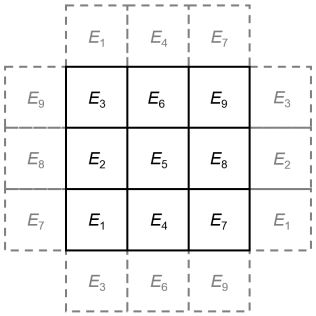

Figure 5. The square lattice shown for a 3×3 periodic mesh with the electric field at each position labeled E_n.

The 2D photonic band structure was calculated for the TM mode of the square lattice GaAs model and is plotted in Figure 6 next to the FEM solution. The photonic band structure result was found to agree with existing results [30].

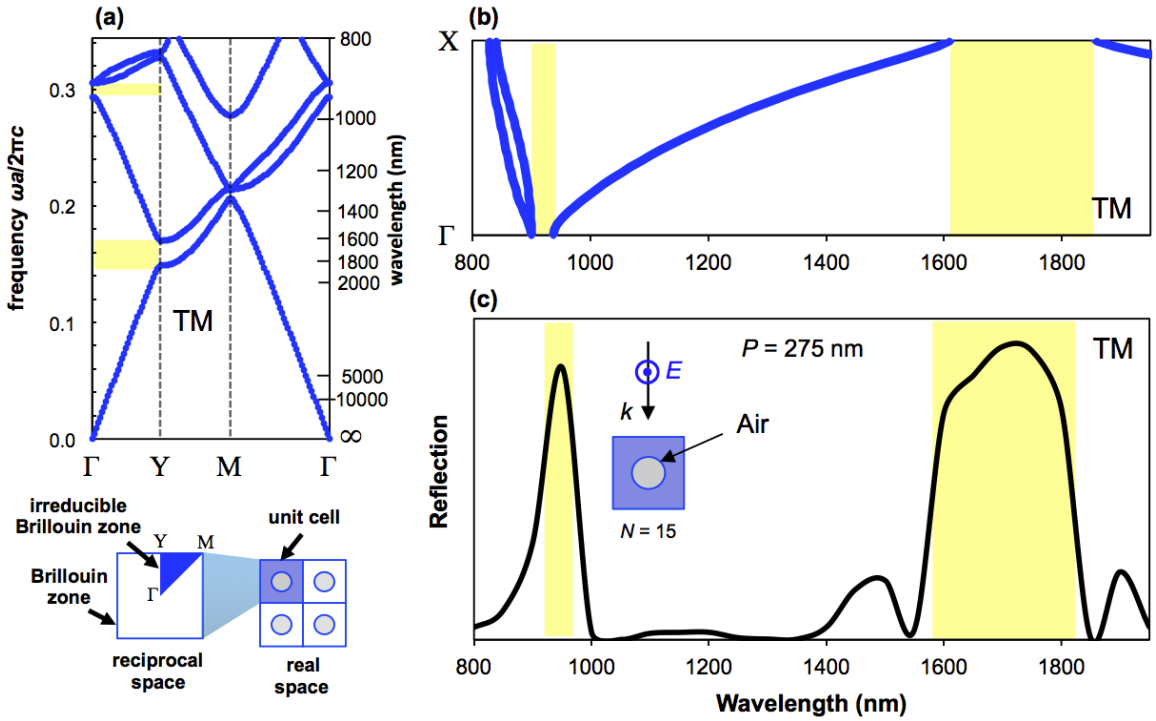

Figure 6. (a) Photonic band structure with unit cell shown in real space and the Brillouin zone and irreducible Brillouin zone shown in reciprocal space. Band structure is for square lattice with air holes in GaAs and with TM polarization. Dielectric constant of 11.8 (b) plots the band structure corresponding to normal incident light parallel to the square lattice as a function of wavelength for the parameters shown: air holes in GaAs, TM polarization, $P = 275$ nm.

5. CONCLUSIONS

A flexible model was designed to evaluate reflection and PBG of a square lattice photonic crystal waveguide under different conditions. The results showed that by increasing the number of layers, the reflection of incident light was increased. TE and TM modes were used under different conditions. Air holes in a GaAs slab were simulated as well as GaAs posts surrounded by air. Modes have different PBG wavelength ranges and reflection peaks for short and long wavelengths. Changing the materials changed the PBG wavelength range and reflection amplitude in short and long wavelength ranges. The period of posts was shown to have a direct effect on shifting the PBG from a short wavelength range to a wider peak.

It has been also determined that using block copolymers for photonic crystals can be challenging. The main limitation at this point is that the typical period of block copolymer structures is too small for PCs that would operate in the visible wavelength region. For GaAs PCs, lower wavelengths will be absorbed in the GaAs, therefore, further future work will be needed to investigate other materials.

REFERENCES

[1] S. Maktoobi, "Analysis and Simulations of Photonic Crystals in Order to Reduce Losses in Photonic Crystal Fibers," *Int. J. Eng. Tech. Res. IJETR*, vol. 2, no. 5, pp. 282–285, 2014.

[2] L. Marko, Y. Tomoyuki, and S. Axel, "Low-threshold photonic crystal laser," *Appl. Phys. Lett.*, vol. 81, no. 15, 2002.

[3] I. Schnitzer, E. Yablonovitch, A. Scherer, and T. . Gmitter, "The Single-Mode Light-Emitting-Diode," *Nano ASI*, vol. 308, pp. 369–378, 1993.

[4] G. Shambat, B. Ellis, A. Majumdar, J. Petykiewicz, M. A. Mayer, T. Sarmiento, J. Harris, E. E. Haller, and J. Vučković, "Ultrafast direct modulation of a single-mode photonic crystal nanocavity light-emitting diode," *Nat. Commun.*, vol. 2, p. 539, Nov. 2011.
[5] V. Berger, "Nonlinear Photonic Crystals," *Phys Rev Lett*, vol. 81, no. 4136, Nov. 1998.
[6] A. Kavokin, G. Malpuech, A. Di Carlo, and P. Lugli, "Photonic Bloch oscillations in laterally confined Bragg mirrors," *Phys Rev B*, Feb. 2000.
[7] B. Bakir.B, C. Seassal, X. Letatre, and P. Viktorovitch, "Surface-emitting microlaser combining two-dimensional photonic crystal membrane and vertical Bragg mirror," *Appl. Phys. Lett.*, vol. 88, no. 8, 2006.
[8] M. Qiu, M. Mulot, M. Swillo, and B. Jaskoryznska, "Photonic crystal optical filter based on contra-directional waveguide coupling," *Appl. Phys. Lett.*, vol. 83, no. 5121, 2003.
[9] M. Qiu, "Ultra-compact optical filter in two-dimensional photonic crystal," *Electron. Lett.*, vol. 40, no. 9, pp. 539–540, 2004.
[10] G. Shambat, M. S. Mirotznik, G. Euliss, and V. O. Smolski, "Photonic crystal filters for multi-band optical filtering on a monolithic substrate," *J. Nanophotonics*, vol. 3, no. 031506,2009
[11] E. R. Brown and E. R. Parker, "Radiation properties of a planar antenna on a photonic crystal," *Opt. Soc.*, vol. 10, no. 2, 1993.
[12] A. Berzezinski, "Engineering and characterizing light-matter interaction in photonic crystal," Degree of Doctor of Philosophy in Materials Science and Engineering, University of Illinois, Urbana-Champaign, 2010.
[13] S. C. J. M., B. H., and O. S., "Low-loss channel waveguides with two-dimensional photonic crystal boundaries," *Appl. Phys. Lett.*, vol. 77, no. 18.
[14] L. O. Faolain, X. Yuan, D. McIntyre, T. S., C. H., and D. L. R. R.M., "Low-loss propagation in photonic crystal waveguides," *Electron. Lett.*, vol. 42, no. 20063077,2006
[15] C. Jamois, R. B. Wehrspohn, J. Schilling, F. Muller, R. Hillebrand, and W. Hergert, "Silicon-based photonic crystal slabs: two concepts," *IEEE J. Quantum Electron.*, vol. 38, no. 7, pp. 805–810, Jul. 2002.
[16] D. Dai and S. He, "A silicon-based hybrid plasmonic waveguide with a metal cap for a nano-scale light confinement," *Opt. Express*, vol. 17, no. 19, p. 16646, Sep. 2009.
[17] M. J. A. D. Dood, E. Snoeks, A. Moroz, and A. Polman, "Design and optimization of 2D photonic crystal waveguides based on silicon," *Opt. Quantum Electron.*, vol. 34, no. 1–3, pp. 145–159, Jan. 2002.
[18] Y. Xu, H.-B. Sun, J.-Y. Ye, S. Matsuo, and H. Misawa, "Fabrication and direct transmission measurement of high-aspect-ratio two-dimensional silicon-based photonic crystal chips," *J. Opt. Soc. Am. B*, vol. 18, no. 8, p. 1084, 2001.
[19] S. Ossicini, L. Pavesi, and F. Priolo, "Silicon-Based Photonic Crystals," in *Light Emitting Silicon for Microphotonics*, Springer Berlin Heidelberg, 2003, pp. 227–262.
[20] L. Pavesi and D. J. Lockwood, *Silicon Photonics*. Springer Science & Business Media, 2004.
[21] J. Mishler, P. Blake, A. J. Alverson, D. K. Roper, and J. B. Herzog, "Diatom frustule photonic crystal geometric and optical characterization," *SPIE Nanobiosystems Process. Charact. Appl.*, vol. 9171, 2014.
[22] T. Fuhrmann, S. Landwehr, M. E. Rharbi-Kucki, and M. Sumper, "Diatoms as living photonic crystals," *Appl. Phys. B*, vol. 78, no. 3–4, pp. 257–260, Feb. 2004.
[23] V. L. Wlech and J. . Vigneron, "Beyond butterflies—the diversity of biological photonic crystals," *Opt. Quantom Electrons*, vol. 39, no. 4–6, pp. 295–303, 2007.
[24] M. Saba, M. Thiel, M. D. Turner, S. T. Hyde, M. Gu, K. Grosse-Brauckmann, D. N. Neshev, K. Mecke, and G. E. Schröder-Turk, "Circular Dichroism in Biological Photonic Crystals and Cubic Chiral Nets," *Phys. Rev. Lett.*, vol. 106, no. 10, p. 103902, Mar. 2011.
[25] J. W. Galusha, L. R. Richey, M. R. Jorgensen, J. S. Gardner, and M. H. Bartl, "Study of natural photonic crystals in beetle scales and their conversion into inorganic structures via a sol–gel bio-templating route," *J. Mater. Chem.*, vol. 20, no. 7, pp. 1277–1284, Feb. 2010.
[26] T. Liu, A. R. Zakharian, M. Fallahi, J. V. Moloney, and M. Mansuripur, "Design of a compact photonic-crystal-based polarizing beam splitter," *IEEE Photonics Technol. Lett.*, vol. 17, no. 7, pp. 1435–1437, Jul. 2005.
[27] S. G. Johnson, S. Fan, P. R. Villeneuve, J. D. Joannopoulos, and L. A. Kolodziejski, "Guided modes in photonic crystal slabs," *Phys. Rev. B*, vol. 60, no. 8, pp. 5751–5758, Aug. 1999.
[28] T. R. Woliński, S. Ertman, A. Czapla, P. Lesiak, K. Nowecka, A. W. Domański, E. Nowinowski-Kruszelnicki, R. Dabrowski, and J. Wójcik, "Polarization effects in photonic liquid crystal fibers," *Meas. Sci. Technol.*, vol. 18, no. 10, p. 3061, Oct. 2007.
[29] A. Urbas, R. Sharp, and Y. Fink, "Tunable Block Copolymer/Homopolymer Photonic Crystals," *Adv Mater*, vol. 12, no. 11, 2000.

[30] J. D. Joannopoulos, S. G. Johnson, J. N. Winn, and R. D. Meade, *Photonic Crystals: Molding the Flow of Light*, Second edition. Princeton: Princeton University Press, 2008.
[31] P. Contu, C. Van der Mee, and S. Seatzu, "Fast and effective finite difference method for 2D photonic crystals," *Commun. Appl. Ind. Math.*, vol. 2, 2011.